■ 889

Fuzzified Single Phase Automatic Sequential Reactive Power Compensation with Minimized Switches

K. Shashikumar*, C. Venkataseshaiah, K. S. Sim
Multimedia University, Faculty of Engineering, Cyberjaya, Malaysia.
*Corresponding author, e-mail: shashikumar@mmu.edu.my, venkataseshaiah@mmu.edu.my,
kssim@mmu.edu.my

Abstract
The current rapid growth in IoT technology facilitates the effortless implementation of bidirectional remote monitoring and control system implementation in homes and buildings. We have modeled an actual non-intrusive PnP sequential SVC prototype hardware and wireless FLC automation software design on a real single phase home appliances system as load modeling. In addition, we have also designed a novel Unidirectional MOSFET Switched Capasitor model (UniMosSC) which enables us to reduce the hardware cost and increase the life span of SVC due it uses minimum switching devices. The system we have designed is able to correct the power factor at the root of the problem at each appliance. Due to complexity of appliance clustering and overlapping clusters, we implemented fuzziness in the system for more reliability in computations. The system could be used in homes or buildings resulting in electricity bill reduction, saving dollars and cents.

Keywords: sequential compensation, SCV, TCR-TSC, FLC, smart meter

1. Introduction

Metering utility and reactive power compensation is essential in power system. The various check points for utility metering and compensation starts from the power plant generation, transmission grid end point, substations, cluster of buildings and finally at each end points of homes or buildings. This is the a standard protocol for some time now. But the emergence of IoTs created the need for more depth in the check points for utility metering, giving birth to Smart Meters with the depth of metering up to each consumer end device appliance. Smart Meters can produce as itemized utility billing for homes or buildings and furthermore help the consumer plan their utility management in line with today's needs for demand management, saving money for consumers.

Our paper here also emphasize more depth in check points for reactive power compensation, to the depth up to consumer end device appliances level for benefits of power quality and consumer's cost saving on utility billing.

To find a proper solutions for a problem, we must dig the roots and not read superficially. The root of the problem lies on the summation of all the numerous small inductive end device appliances causing the reactive nature on the overall power grid system. Although with large reactive power compensator installed all over utility providers grid system, the utility providers are constantly blaming the owners of the buildings and imposing heavy penalties and fines to solve reactive power issues. The problem could be resolved with our automatic sequential reactive power compensator system installed in every end device appliance and monitored remotely by the utility provider rather than the building owner for best compensator result for the their power gird. Rather than controlling appliance as suggested by this paper [1], we have improved with adding compensator at each end device.

Our paper here shows a working prototype for utility providers or building owners to emphasize on reactive power compensation at the root of end device load than just preforming the action at the mains of the building alone which it is not sufficient enough. Our prototype is small in size, cost efficient and easily PnP to existing IoT systems where security is essential [2]. We have designed the system and tested on a single phase power system in a home environment with promising results. The system could be extended to a large quantities of three

phase end load devices in a large residential or industrial building with renewable energy sources [3].

Our system also design with less switching devices used reducing the THD level from the conventions systems. We have also used FLC for appliance clustering increasing calculation speed and decision making. Use of FLC in our system also makes it easy for humans or a programmer to visualized and re-model the system.

2. Software Implementation

There are many works related to load profiling of home appliance power or current readings from the utility mains meter box. Rather than profiling the load at the mains, our previous design a novel alpha numeric appliance ID Tag architecture system [4],[5] has been further improved to a simpler percentage digits Tag ID table as shown in Table 1. We have clustered home appliance according to load type and operation mode type before Tag ID assigned for each appliance as shown in Table 1. Our non-intrusive load meter and load corrector hardware is embedded with Tag ID signal from the Table 1 for each end device appliance in the home. The Tag ID will help the main server to decide the priority order in home utility compensation system.

Tables 1. Classification of Home Appliance with Digital Tagging ID Digits Interconnected with Compensation Priority

Load Type & Cluster	Cap.Loads	Resistive Loads			Electronics Loads				Inductive Loads			Total / Main Meter & ELCB Box
	Fix	Portable	Existing	Fix	Portable	Existing		Fix	Portable	Existing	Fix	
	Continues	Small	Intermediate	Continues	Small	Intermediate		Continues	Small	Intermediate	Continues	
Appliance	—	⬛🔲▲	⬛▦◩◪	🕯	◰📱	🔦▃◥◣⬛◈▦◪▦◨		🕯	🔦📱📲	▦🍴📟◼◼	✳◨	▦▦
Tag ID	0.0	0.05	0.1	0.15	0.2	0.25 0.3 0.35 0.4		0.45	0.5	0.6 0.7	0.8 0.9	1.0

Fuzzy Logic Controllers is widely implemented in SCV systems. Authors of paper [11] illustrates the use of FLC in optimizing SVC-Dual-TCR-FC Thyristor firing angles relative to input of load phase angle difference. Whereas paper [12] also illustrates the use of FLC in SVC-Dual-TCR-FC Thyristor firing angles as input functions of load relative power variations. Both papers findings is that the useful firing angle for TCR is between $110°<α<170°$ as of best results.
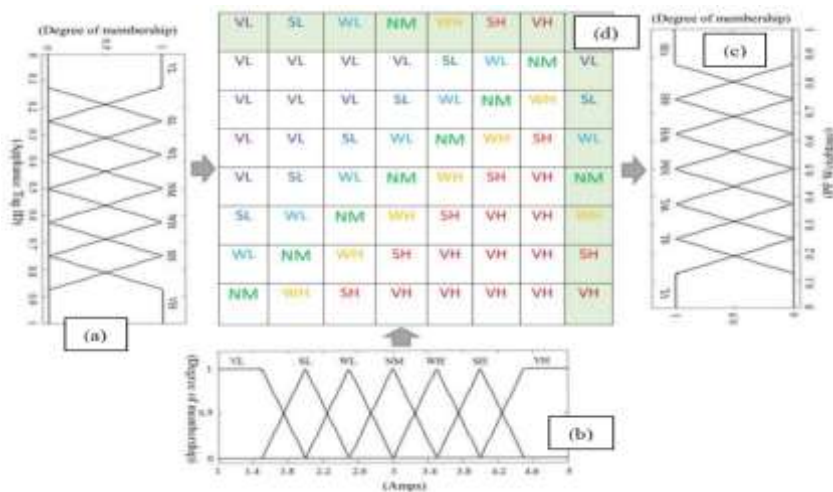

Figure 1. (a) and (b) shows the both inputs of fuzzy subsets , Figure 1 (c) shows the output of fuzzy domain, Figure 1 (d) shows the rules tabled

From our work in paper [5] we have created a set of if-else rules to choose the highest priority appliance cluster for Stepped Sequential MSC Binary PFC. For this paper we have improved the our previous system with a fine tuned membership functions for a Mamdani Fuzzy Logic Controller with two inputs and one output system. We have adopted triangle-type membership functions curves of Appliance Tag ID for the first input of the FLC as shown in Figure 1(a) which has fuzzy subset {0.00, 0.25, 0.45, 0.50, 0.65, 0.75, 1.00} which corresponds to {VL, SL, WL, NM, WH, SH, VH}. For the second input of the FLC we have adopted triangle-type membership curves of Appliance Current as shown in Figure 1 (b) which has fuzzy subset of {1.00, 2.0, 2.4, 3.00, 3.36, 4.00, 5.00} which corresponds to {VL, SL, WL, NM, WH, SH, VH}. For the output FLC we have adopted triangle-type membership curves of Wightage for Power Factor (PF) as shown in Figure 1 (c) which has fuzzy domain of {1.00, 2.0, 2.4, 3.00, 3.36, 4.00, 5.00} which corresponds to {VL, SL, WL, NM, WH, SH, VH} stand for very low, strong low, weak low, normal medium, weak high, strong high, and very high, respectively.

The number of fuzzy sets is chosen corresponds to 49 fuzzy rules is implement for the proposed fuzzy Automatic Sequential Reactive Power Compensation. In this paper 49 fuzzy rules as shown in Figure 1(d) considered necessary because less that 49 rules will correspond to blur amount lowering output accuracy and higher from 49 rules will correspond to to many rules slowing the processing. We have not used any specific method for designing the FLC, but to emulate human decision making the input and output membership functions is designed.

The weightage, W value is fed to series of MATLAB calculations as shown on Figure 2 to set the values of Stepped-UniMosSC capacitor banks set and setting the UniMosSC and TSR firing angles. This process repeats itself for each end load appliance from the highest priority appliance to the lowest priority appliance, fine tuning the power factor raising it to near unity. As shown in Figure 2 a priority list is calculated, according to the highest value of appliance Tag ID versus highest current the appliance consumes. This results in equivalent to fuzzified output of weightage, but the main meter Tag ID with weightage at 1 is replaced with weightage at 0 as last priority. The last priority actually does the highest order to compensate to unity or 1pf.

The weightage, W from the fuzzy output ranges from 0 to 1 is used to set the new power factor desired PFdesired, from the measured power factor PF. The weight set in percentage of difference from the measured PF with Unity PF as in Equation (1).

$$X_c = \frac{V^2}{Q_C}$$

(1)

P is the measured true power in kW units. MF is the multiplication factor that calculates the reactive power QC the in kVAR units using Equation (2) and (3). The conventional way would be to use VAR power factor correction chart but Equation (2) and (3) represents the conventional chart in equations for easy computational coding purpose.

$$C = \frac{1}{2\pi f X_c}$$

(2)

$$Q_L + [(20\%)(Q_L)] = \frac{V_{RMS}^2}{X_C}$$

(3)

Then the correction CX capacitor C bank values in μF are used to archive the desired power factor using Equation (4) and (5). Where V is the supply voltage and f is the supply frequency usually around 240V and 50Hz respectively. Xc is capacitive reactances in Ohms.

$$X_{L(TCR)} = \frac{V_{RMS}^2}{Q_L}$$

(4)

$$X_{L(TCR)} = \sqrt{\frac{2(\pi - \alpha) - \sin(2(\pi - \alpha))}{\pi(X_L)}}$$

(5)

When the Matlab Simulink software finishes calculating the CX capacitor values, it then rounds it to the nearest fraction of half. Then the value compared with existing stepped capacitor bank combinations values to set to the nearest possible combination. This is done using a set of if-else instructions derived from our past work [5] Binary PFC. Finally the desired capacitors are triggered at the correct firing angle using UniMosSC. Figure 2 shows the overall process of calculation and the process.

From the Matlab Simulink diagram in Figure 2 it also shows another parallel calculation process done to find the TCR firing angle using the desired reactive power QC. The values of QC converted to XC then QL found using Equation (6). Then the firing angle impedance XL(TCR) calculated using Equation (7) and finally the firing angle α is calculated using Equation (8).

$$L = \frac{X_L}{2\pi f} \tag{6}$$

$$PF_{desired} = \big(1 - (PF)\big)(W) + PF \tag{7}$$

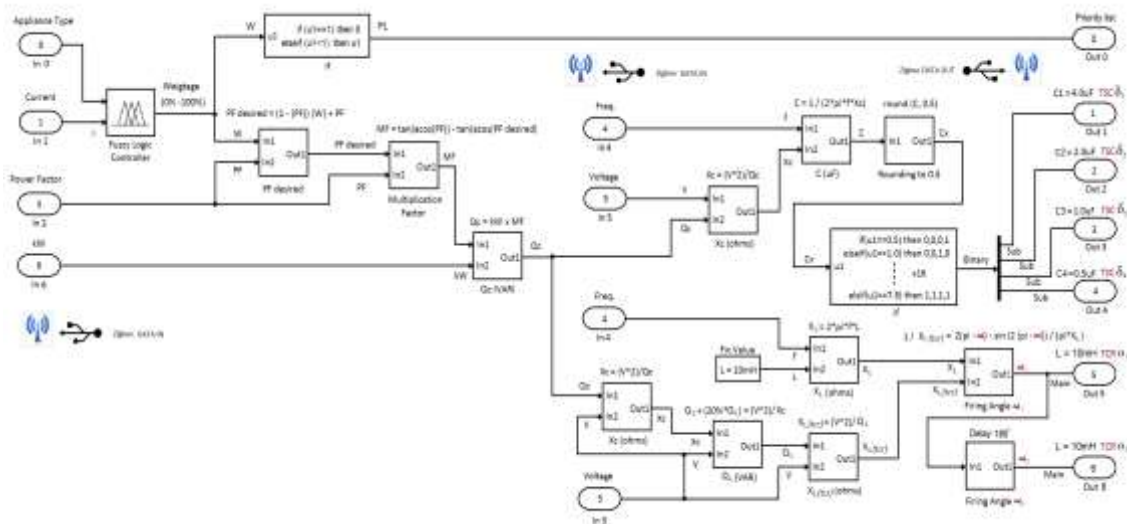$$X_L \leq X_{L(TCR)} \leq \infty \tag{8}$$

Figure 2. The fuzzy surface plot showing the appliance load current and appliance priority tag ID inputs resulting output fuzzified weightage.

The firing angle calculated is for the first half cycle which corresponds between 90°<α<180°. The next half cycle firing angle is calculated by adding 180° as shown in Figure 2. Equation 9 is helpful for choosing the right reactance value from calculated XL(TCR). We have chosen 10mH as its impedance as this value is below the value of XL(TCR) to satisfy the condition in Equation 10.

$$Q_C = (P)(M_F) \tag{9}$$

$$M_F = \tan(\mathrm{acos}(PF)) - \tan(\mathrm{acos}(PF_{desired})) \tag{10}$$

We have chosen 10mH as its impedance as this value is below the value of XL(TCR) to satisfy the condition in Equation 10.

3. Simulations

The MATLAB Simulink model for simulating single phase AC voltage source of 240V 50Hz, is shown in Figure 5. Active power of each parallel load is 880kW and reactive power is 0.24kVAR. The monitor block collects instantaneous current and voltage flowing from source. Scopes place at various positions to display the signals generated during simulation. The real power and reactive power is calculated resulting computation of capacitors and computation of inductive in Figure 5 as similar to illustration of Figure 2 in this paper. Finally this C and L values need to archive recalculate as firing angles.

Figure 3 shows simulated the Dual-TCR controlling the current across the inductor for firing angles is limited to $90° < \alpha < 180°$ for each half cycle.Where else for Dual-MosSC as shown in Figure 4 the conduction angles is limited to $90° < \alpha < 180°$ for each half cycle controlling the capacitor. The duty cycle of Thyristor firing angle is merely 1% of 50Hz supply period resulting to $3.6°$ or 20µs. Where else the duty cycle of MOSFET conduction angle is as large as $90°$or 5ms.
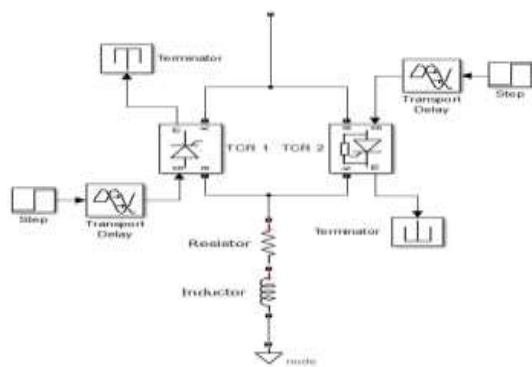

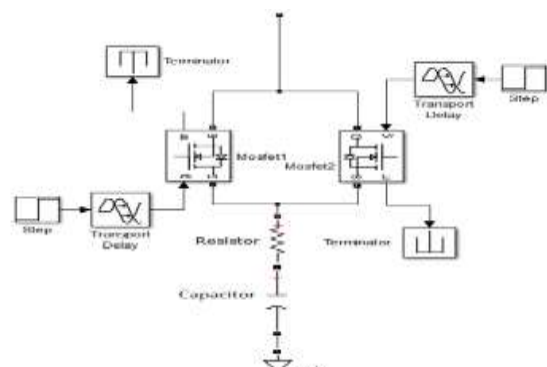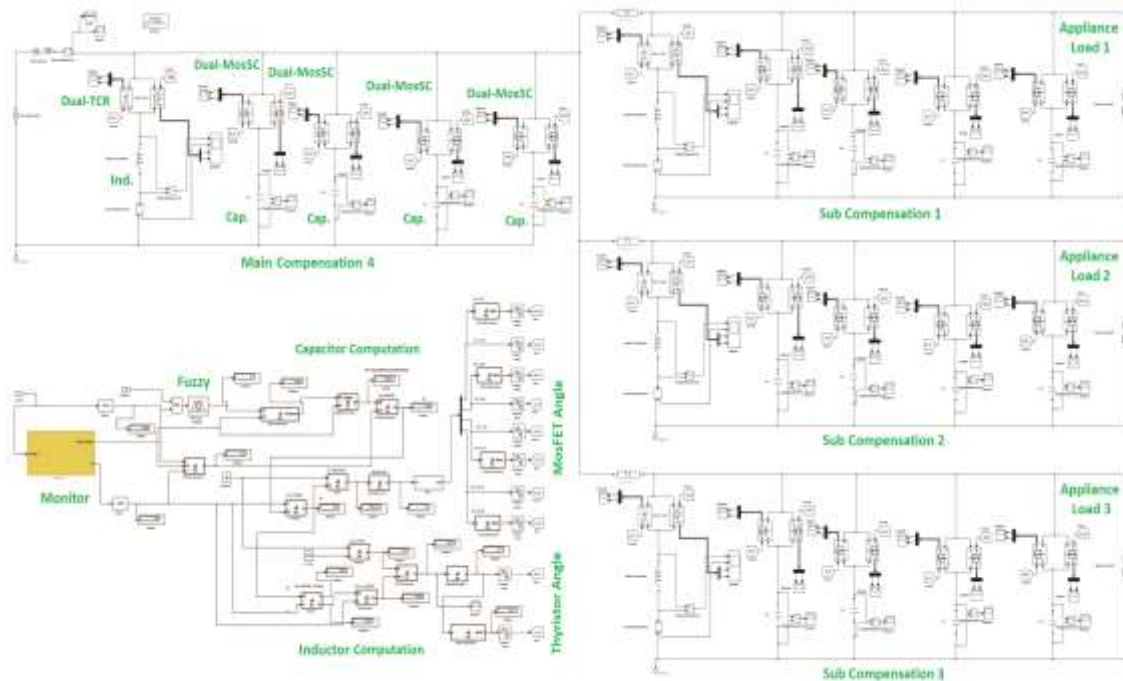Figure 3. shows a Dual-TCR shunt circuit   Figure 4. shows Dual-MosSC shunt circuit

Figure 5. The MATLAB simulink model for Dual-TCR and Dual-MosSC Automatic Sequential Reactive Power Compensation

MATLAB Simulation in Figure 5 configured as SVC with Dual-TCR and Dual-MosSC working as a Fuzzied Appliance Automatic Sequential Reactive Power Compensation. There is three appliance loaded and connected to the system. Each load compensates in sequential according to the appliance weightage and final compensation occurs at mains. Figure 6 show overall power factor measured in the mains during compensating process for each stage in Figure 5. The compensation starts with sub compensation one block at 0.03s, then sub two block at 0.07s, following sub three block at 0.13s and ends with main compensation block at 0.17s. From Figure 6 we could see that there is sequential improvement of power factor from 0.80pf without compensator to 0.98pf after full compensator settled at 0.20s.

From Figure 6 we could also see variations in power factor curving down hill and up hill rather than expected result of simple up hill stair case curve. This effect could be explain easily as due to fuzziness applied in our system, the change of overall current due to effect of compensation at a stage will recalculate the new value of compensating capacitors and reactor, creating a coupling effect between both like a salsa dance between them. In other words the capacitors will keep changing combinations and the reactor follows to its rhythm and keep changing its firing angle. This process oscillates till the minimum capacitor value and maximum firing angle achieved in the reactor at the point of steady current drawn at that stage. After all the rhythmic dance between capacitor and reactor at each stage the system finally halts at 0.20s. The chosen two power factor modeling technique demonstrates the robustness of our fuzzy sequential reactive compensate.
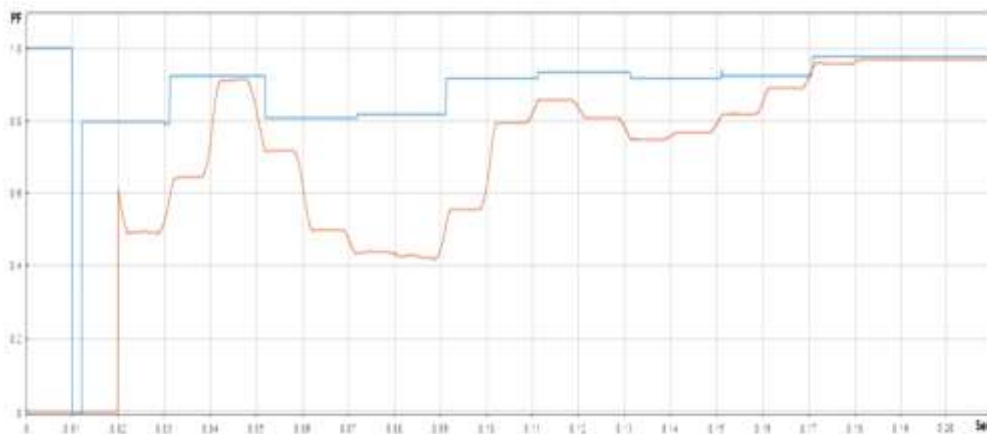

Figure 6. shows both waveform shows PF monitored at the mains versus time. The blue waveform shows accurate PF using power factor measurement block, where else the red waveform calculates PF using integral power factor modeling technique.

4. Hardware Implementation

One of the essential systems for our Sequential Reactive Power Compensation System is monitoring energy quality and compensation. Basic compensation system design uses combination of Mechanically Switched Capacitor (MSC) banks as illustrated in paper [6]. In our earlier designs we have built multiple units of wireless PF meter and Stepped MSC Binary PFC [5] at each end device appliance load. We have incorporated a similar design concept in our Stepped MosSC topology Sequential Reactive Power Compensation System for this paper but instead of using MSC relay devices, we have used semiconductor switches MOSFET. For SVC implementation the major hardware component is the Thyristor. Correct combinations of driver and microcontroller should be used for reliable hardware implementation. Paper [13]-[14] and [15] illustrates on fully functional shunt SVC circuitry and hardware building.
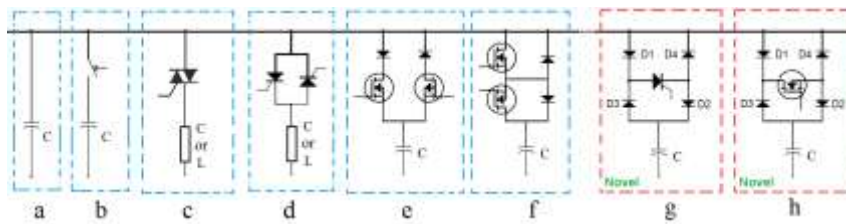
Figure 7. types of switching models used for capasitive and reactive compensators. the right combinations of Switching models SVC topology can be created. a) FC b) MSC c) TriacCR or TriacSC d) Dual-TCR or Dual-TSC e) Dual-MosSC f) SSR-SC g) Our Novel UniTSC h) Our Novel UniMosSC

Shunt SVC can be of the following types SVC-TCR-FC or SVC-TCR-MSC or SVC-TCR-TSC as shown in Figure 7. For a SVC, TCR is combined with any of the combinations in Figure 8 with Fix Capacitor, Mechanical Switched Capacitor, Thyristor Switched Capacitor or with Solid State Relays Switched Capacitor models. In this paper we have designed a new novel topology of SVC-TCR-UniMosSC a Thyristor Controlled Reactor with Unidirectional MOSFET Switched Capacitor topology that only uses one switching device, reducing the cost of the system and mitigates control malfunction or wrong time switching.

One of the drawbacks of the SVC system is that it's switching devices produces comparatively high harmonic distortion in the power lines as illustrated in paper [7] a Dual-TCR topology with firing angle is $95°$ and $275°$ resulting in a typical 0.51 THD for a single phase system. Paper [8] illustrateds a SVC-Dual-TCR-FC topology with firing at $140°$ and $320°$ for a 0.5mH inductor and capacitor choice of 5uF to compensation capacitor values of 4.887uF. Authors of paper [9] designed a SVC-Dual-TCR-Stepped-TSC with multi banks of Thyristor switch capacitors combinations used.

In a shunt SVC system the TSC is not used to control the value of capacitor as it is done with TCR, but merely just to ON or OFF the TSC bank capacitors [7]. In contrast, in TCR the control of inductor value is achieved by controlling the current across inductor resulting in variation of the QL. For TCR the Thyristor firing angles is limited to $90°<α<180°$ for each half cycle, where else for TSC the MOSFET conduction angles is limited to $0°<δ<90°$ for each half cycle and any firing angle larger $90°$, face step inrush currents or trapped charge in the TSC capacitor.

Our UniMosSC, works on single line 100Hz switching frequency controller fed to MOSFET gate but Dual-TSC works on dual line dual 50Hz switching frequency controller fed to each Thyristor gate. TSC works on short burst of pulse that once activated the Thyristor it will only be switched OFF when the current drops to zero. Whereas in our MosSC device, large pulse is used resembling the conduction angle and it is supplied for both half cycles.

The advantage of our UniMosCS topology is that it uses only one switching device and one gate drivers circuit. Another advantage in our design is that the conduction angle starts at the point of zero crossing entry whereas in Dual-TCR there is a need for delay between both signals increasing error propensity. The control signal for UniMosCS is easy to operate and it reduces errors in switching time to the MOSFET.

The UniMosCS topology in Figure 7 works with MOSFET permitted to flow in sections of the first positive half cycle of line supply with D1 and D2 in forward. At each cycle only one way the direction of current flow, from drain to source. The choice of using Thyristor or MOSFET model largely depended on the end device loads and the electrical system Thyristor used for three phase and MOSFET used for single phase system.
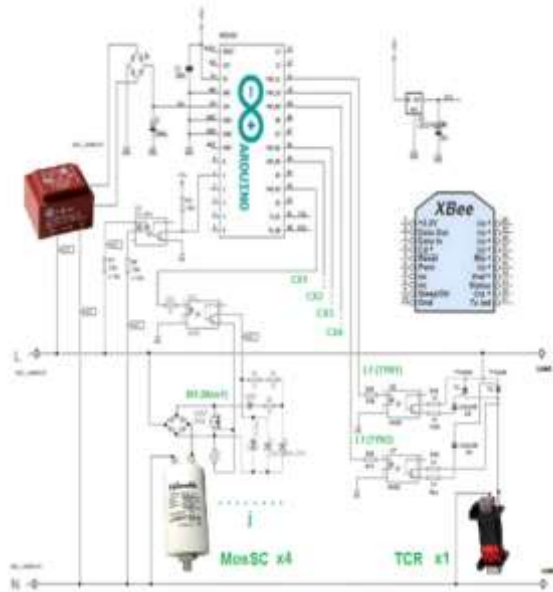
Figure 8. circuit design for a non- intrusive SVC compesation system with a TCR and with four Stepped CX binary MosSC System
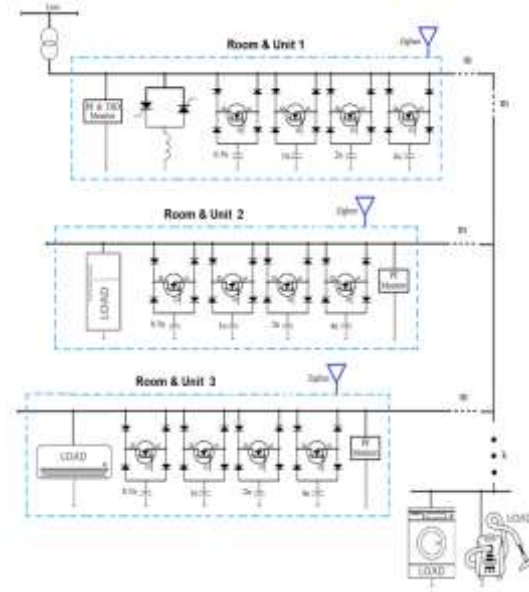
Figure 9. our overall block diagram hardware system design implementation on a single phase system in a home

Figure 8 shows our single phase SVC System circuit design. The circuit uses Myrra PCB though hole transform 9Vac, 2.5VA, 50Hz for the system 5V an 3.3V DC power supply, IC ATmega 328p and Zigbee. For power line 240V, 50Hz zero crossing detection we use is IC H11AA1. XBee Series 2, Part number XB24Z7WIT-004 is used for communication to the main server. The ATmega microprocessor we have assigned has six PWM digital pins as output to switching devices.

Two digital pin signals is used for TCR module. They are connected to two different optocoupler 4N25 as an isolation gate driver to two Thyristor TYN404 modules (rating 400V, 4A). Both Thyristor are connected with a shunt core inductor of 18AWG, 10uH.

The ATmega's another four digital pin signals are used for TSC module. Each digital pin signal is connected with an optocoupler 4N25 as an isolation to the gate of the MOSFET's IRF830 (rating 500V, 4.5A) and the high voltage circuity that biases to the MOSFET gate and the bridge rectifier power diodes. This four UniMosSC repeated modules is connected to shunt CX capacitors each with values of 4uF, 2uF, 1uF and 0.5uF creating a Stepped-UniMosSC topology.

Our non-intrusive SVC System hardware in Figure 8 is installed closed to the single phase main box of Room 1 or the living room of a home as shown in Figure 9. PF meter and THD meter we have built in previous paper [5] are also installed in Room 1 and all are controlled and monitored via Zigbee wirelessly via a server.

Additional units 2, 3, 4 and 5 are installed in the same home approximately close to inductive end device appliances; refrigerator air conditioner, washing machine and vacuum cleaner respectively. Each of this unit consisted only our Stepped Binary UniMosSC and PF meter via wireless Zigbee communication to the same server. The appliance is connected to the main utility around 100 feet apart with 10AWG copper wires as shown in Figure 10 with variable of m in meters. The internal resistance of the wires is 0.1 ohm resistance per 100 feet. The number of appliances can be increased and set as variable k. The wireless Zigbee communication with the server and k number of units is connected in request mode than timely manner broadcasting mode method because to reduce the tendency of congestion in wireless network queuing. In other words the communication is controlled by the server requesting for monitored data or controlling access with the other nodes of Zigbee in the system.

5. Results

The yellow spikes signals in Figure 10 and Figure 11 are observe waveform from oscilloscope measured at zero crossing output. Where else waveform measured in between 10mH inductor and Dual-TCR shown in Figure 10 for firing angle setting at 110˚ and 290˚. Figure 11 shows the oscilloscope waveform measured in between CX capacitor and UniMosSC at conduction angle setting of 90˚ and 270˚.

We have complied and plotted three different results from our Sequential Reactive Power Compensation System as shown in Figure 12.

Multi-Stepped-UniMosSC compensator where only Stepped UniMosSC is used though out the sequential compensation system resulting the final phase angle of 0.95pf and harmonics measurement of 5.9 THD.

Multi-Stepped-UniMosSC and Single-Dual-TCR compensator where Stepped-UniMosSC is used though out in all the end appliance devices and in the final sequential compensation stage both MosSC and Dual-TCR combination are used resulting in the final phase angle of 0.97pf and harmonics measurement of 6.7 THD.

Multi-Stepped-UniMosSC and Multi-Dual-TCR compensator where Stepped-UniMosSC is used though out in all the end appliance devices and at the same time Dual-TCR at the main box is also switched for each sequence of Stepped UniMosSC switching resulting in the final phase angle of 0.99pf and harmonics measurement of 6.8 THD thus giving the best results of PFC for our system.

The system operation order is of the flowing sequence-once our single phase Sequential Reactive Power Compensation System is activated, the coordinating server collects the appliance priority list and weightage which it is used to calculate the capacitor combination needed. Then at the end device appliance where the UniMosSC compensator is connected, the desired capacitor combination is triggered via turn on the MOSFTEs and at the same time firing angle for TCR compensator is calculated and triggers at the main electrical box.

Upon first sequential execution at the refrigerator appliance the program will find the next highest priority order appliance and repeat the process with a lesser weightage compensation. For our system, the second periodically ordered sequential appliance is the air conditioning. The process interval of 5 seconds is given for each sequential for the system to enquire data wirelessly, processing calculation, hardware execution and compensating transient relaxation. Repeatedly the cycle continued to lower priority order with lower compensation weightages improving the total PF phase angle of the overall home utility system as in Figure 13. The final compensation was performed at the main electrical box with the highest weightage of one to compensate the final brew of reactive power. Our system kicks on reset mode if the system detects the phase angle drop below 0.9pf or the total load current drop drastically below 75% at the main electrical box.

The final sequential compensation happens at the main electrical box itself, where we have set it to the lowest priority but the highest weightage at a given point of time of unity. The final brew compensated at this point is near unity PF phase angle.
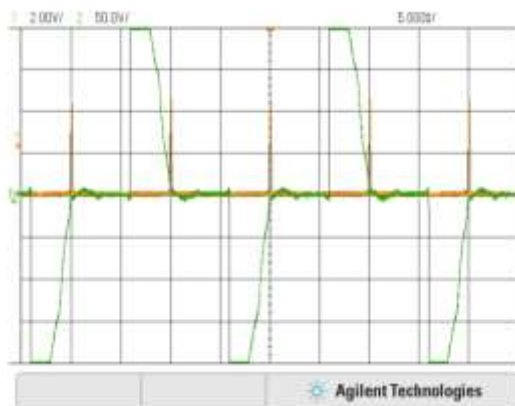

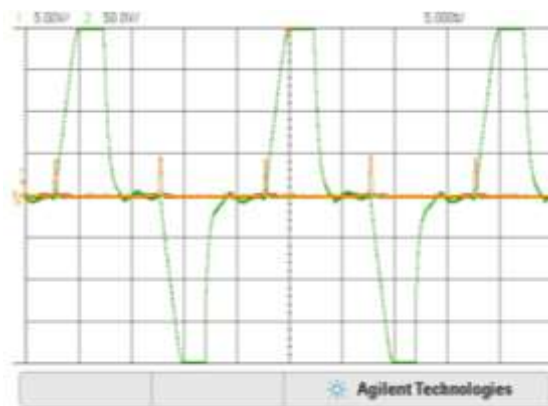Figure 11. shows Dual-TCR firing angle   Figure 12. UniMosSC conduction angles
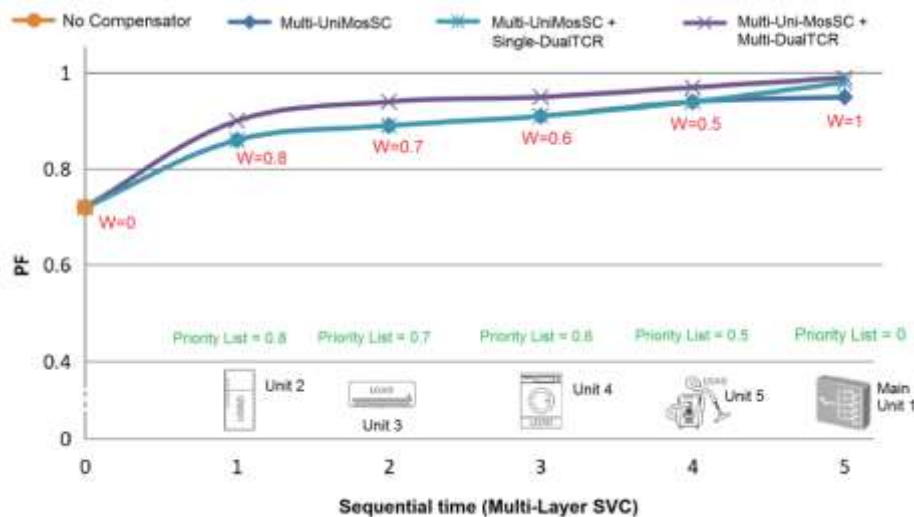
Figure 13. shows PF reading we have observed and plotted at different situations and placements of Stepped-UniMosSC and Dual-TCR compensating system. It also shows the thyristor triggering angle and capacitor tuned values used at each sequence.

6. Conclusion

Our non-intrusive plug and play Sequential Reactive Power Compensation system is easily installed in any building without additional wiring required. Furthermore the hardware system compensates approximately unity which translates to reduction in consumer utility billing. The complexity of appliance clustering computations done quickly by our server with simplified fuzziness implementation. The UniMosSC gate control signals of our system is pro error redundant and further we have reduced the units we use for the gate driver and switching devices resulting THD noise suppression and in reduction of hardware production cost.

Our system has capacitor banks being equally distributes throughout the building electrical system compared to the conventional system of having one big bank of capacitors at the main electrical box. This distribution of capacitor bank adds in advantages:
a. It is space saving as smaller size PFC installed and distribute evenly throughout the building.
b. It solves power quality issue at the root of the problem achieved.
c. It acts as early warning detection of end appliance power leakage drain or fault.
d. It is robust as if one of the PFC end device module fails other PFC module replaced its role compare to the current PFC modules where the failure of PFC module fails the overall system at home level.

Our system has multiple PF monitoring and PFC nodes with reliable wireless communication connected to home server. Adds in Advantages:
a. Remote monitoring and controlling end device home PFC nodes by the utility provider.
b. Transferring the cost of PFC at feeder end which is consumed by the utility provider to consumer level.
c. Consumers could analyze their behavior of their home for better energy management.
d. Utility provider could analyze consumer behavior for better management of dynamic PFC grid system.

We did not expand our system to a large industrial building and did not further enhance the system for three phase appliances, due to financial constraint. Further for enhancement of our system it requires huge amount of funds. For future work, we would recommend research to be done on SSR-SC models and UniTSC topology.

Reference

[1] R Dorothy, et al. Smart Grid Systems Based Survey on Cyber Security Issues. *Bulletin of Electrical Engineering and Informatics (BEEI)*. 2017; 6(4): 337-342.

[2] Sabriansyah Rizqika Akbar, et al. Home Appliance Control with Publish Subscribe Social Media. *(TELKOMNIKA) Telecommunication, Computing, Electronics and Control.* 2015; 13(2): 678-685, 2015.

[3] Bhupendra Sehgal, et al. Performance of FACTS Devices for Power System Stability. *Indonesian Journal of Electrical Engineering and Informatics (IJEEI)*. 2015; 3(3): 135-140.

[4] Shashikumar K, et al. *Juggling an Arduino for Multi-Meter, Load Profiling and Novel Waveform Capture Logger Application*. 12th International Colloquium on Signal Processing & its Applications of IEEE. 2016: 119-123.

[5] Shashikumar K, et al. *Automatic Sequential Reactive Power Compensation and Harmonic Suppression at Loads using Appliance Clustering and Power Quality Monitoring*. International Conference on Robotics Automation and Sciences (ICORAS) of IEEE. 2016: 1-6.

[6] M Anjana Shree et al. *Smart Meter for Power Factor Enhancement in Real-Time.* IEEE International Conference on Embedded System (ICES). 2014: 177-181.

[7] G Tapia et al. *Comparative Time Domain Modelling and Analysis of a Single-Phase TCR*. IEEE Electronics Robotics and Automotive Mechanics Conference (CERMA). 2007: 663-668.

[8] Taufik et al. *A small scale Static VAR Compensator for laboratory experiment*. IEEE 2nd International Power and Energy Conference. 2008: 1354 - 1357.

[9] A Nader Barsoum et al. *Programming of PIC Micro-Controller for Power Factor Correction*. IEEE Conference on Modelling & Simulation (AMS). 2017: 19-25.

[10] Pieter Schavemaker et al. Electrical Power System Essentials. Publisher Wiley. 2008:158.

[11] S Zemerick et al. Design of a Microprocessor Controlled Personal Static VAr compensator (PSVC). *IEEE Power Engineering Society Summer Meeting*. 2002: 1468-1473.

[12] S Khanmohammadi et al. *Fuzzy Logic Based SVC for Reactive Power Compensation and Power Factor Correction*. IEEE International Power Engineering Conference (IPEC). 2007: 1241-1246.

[13] Mohammed Imran, et al. *Designing of Phase Angle Control and ON-OFF Triggering Circuit for SVC Reactive Power Compensator*. IEEE International Conference on Electrical, Electronics and Optimization Techniques (ICEEOT). 2016: 1763-1768.

[14] Md. Ruhul Amin et al. *Design of microcontroller based Thyristor Controlled three-phase static volt-ampere reactive compensator*. IEEE International Conference on Informatics Electronics & Vision. 2014: 1-6.

[15] Manan Y, et al. *Design and Hardware Implementation of SVC using Thyristorised Control for improving power factor and voltage profile of inductive loads*. IEEE 6th International Conference on Power Systems. 2016: 1-6.